Shape-Sensitive Linewidth Measurements of Resist Structures

LITG410I Project

Submitted to International SEMATECH

by

John S. Villarrubia
Model-Based Linewidth Project Leader

András E. Vladár
SEM Project Leader

Michael T. Postek
Nano-Scale Metrology Group Leader

National Institute of Standards and Technology
100 Bureau Dr.
Gaithersburg, MD 20899-8212

TABLE OF CONTENTS

Certain commercial products are identified in this report in order to describe the experimental and analytical procedures adequately. Such identification does not imply recommendation or endorsement by NIST, nor does it imply that the equipment identified is necessarily the best available for the purpose.

EXECUTIVE SUMMARY

Scanning electron microscopes (SEMs) are widely used to take images and make dimensional measurements on resist and polycrystalline silicon ("polysilicon") lines fabricated on Si wafers. SEM images generally show these lines with characteristically bright edges. Much of the uncertainty in linewidth or critical dimension (CD) measurements is due to the fact that the bright regions that represent a line's (or gate's) edge in a SEM micrograph are not sharp at the nanometer scale. Each edge "zone" may be tens of nanometers wide, and the variation of image intensity within this region depends upon characteristics of the edge shape and instrument parameters.

The National Institute of Standards and Technology (NIST) has been developing a CD measurement method, the model-based library (MBL) approach that works analogously to optical scatterometry. Once an image comprised of a series of line scans is collected, a model-based library is searched and interpolated for a match to the measured image. Because it is based upon a physical model of the electron scattering process in the line, MBL SEM metrology is potentially more accurate than the traditional methods. In previous projects we have demonstrated good agreement between MBL SEM and cross-sectional SEM on polysilicon samples.

The present study extends these comparisons to industrially important resist samples. Because resist is an insulator, charging of the sample is potentially an obstacle to good dimensional metrology using MBL SEM or any other SEM-based technique. Additionally, some properties of resist that are needed for modeling it are poorly known. It was not known at the inception of this project whether these issues represent only annoyances or insurmountable obstacles to good CD metrology.

The samples employed were fabricated at International SEMATECH (ISMT) from the AMAG4L reticle. This reticle includes linewidth test patterns that were designed at NIST. These patterns were exposed and developed in PAR-810 resist. They were subsequently imaged top-down in the Applied Materials NanoSEM at ISMT, after which they were cross-sectioned and imaged again using a laboratory SEM. Cross-section/top-down image pairs were successfully obtained for 48 different targets, each of which consisted of three to ten lines of nominal width 100 nm, 200 nm, or 350 nm.

These image pairs were analyzed at NIST using modeling to determine edge profiles from both the top-down and cross-section images. Differences between the two measurement methods had a standard deviation of approximately 5 nm. Linewidth roughness accounts for 3 nm of this. The MBL-determined linewidths averaged 3.5 nm larger than the cross-section determined ones. Since the cross-sectioned samples received a larger electron dose, resist shrinkage could be responsible for the difference. This difference is also within the uncertainty of determining line edges from the cross-section images, the main source of which is the sensitivity of cross-section edge determinations to the divergence angle of the SEM's electron beam (which is responsible for the instrument's finite depth of field). This sensitivity, which we discovered in the course of modeling for the cross-section edge assignments, has not heretofore been adequately appreciated.

These results indicates that the adverse influence of charging on MBL dimensional measurements of resist is bounded at the observed level of a few nanometers for resist samples measured under conditions like those we employed. They may possibly be less since other adverse influences could account for some or all of this difference.

1 INTRODUCTION

A microscope image is an imperfect representation of the sample. High resolution microscopes are quite good, but the demands of accuracy placed upon them by the semiconductor industry are very high. At the nanometer and sub

nanometer uncertainty levels being required for current and near-future device generations, important instrument artifacts must be accounted for in the measurement of feature widths. For width determinations with the scanning electron microscope (SEM) an important artifact is the edge bloom that results from electron scattering within the sample and secondary electron production by electrons scattered through a feature's steep sidewalls (Fig. 1). The blooming is what creates the contrast that distinguishes edges from the rest of the sample, but the finite width of the bloom may create tens of nanometers of ambiguity in the edge position. Existing CD-SEM (critical dimension SEM) edge finding algorithms make arbitrary assignments of edge positions. Such arbitrary assignments are made with the knowledge that they will produce a measurement bias (i.e., a nonrandom component of error) and with the hope that the bias will be consistent from sample to sample, thereby leaving measurements of width differences unaffected. The bias inherent in these methods of edge assignment is too large to meet the now very tight accuracy requirements in the ITRS.[1] Recent theoretical[2] and experimental[3] studies suggest that even the assumption of constant bias breaks down at the few nanometer level. The bias may vary from one sample to the next, with the result that commonly used algorithms may contribute several nanometers of error even to measurements comparing one width to another.

To do better requires that we know how the instrument interacts with the sample to produce the image. Such knowledge is embodied in a computational model of the probe-sample interaction—a piece of software that uses known or assumed physics of the interaction to calculate the image that would be observed for a given sample geometry.

With such a model in hand, it is possible to make a more reasonable assignment of edge positions. In the mid-1990s MONSEL, a computational model capable of simulating secondary electron production from linear features using Monte Carlo methods, was developed at NIST.[4] In the last few years International SEMATECH (ISMT) and NIST have cooperatively pursued projects to develop and experimentally validate such models for a case of particular interest to semiconductor manufacturers, SEM images of silicon lines. Cross-sectional profiles of actual polycrystalline Si ("polysilicon") lines or gates may differ in important ways from ideal rectangles. For example, corners may be rounded and sidewalls may not be perfectly vertical (Fig. 2). Determining as many of the shape parameters as possible, including of course the width, is the object of the MBL (model-based library) measurement algorithm developed during the course of these earlier projects.

The principle of operation of the MBL method is illustrated in Fig. 3. The unknown sample is imaged in the SEM. The measured intensity profile at each edge is then compared to a set of profiles previously calculated for a range of edge shapes using MONSEL. By interpolating between profiles in the library, the profile that best matches the measured edge profiles is found. The corresponding edge parameters are attributed to the unknown specimen.

In 2001, comparison of the MBL-determined profiles (based upon images obtained with a laboratory SEM at NIST) with the profiles measured in cross-section gave good agreement for the line's width and the angles of the side walls (Fig. 4). CDs determined by regression to baseline were biased by approximately 15 nm and exhibited more than a factor of 3 poorer repeatability.[7] [8] Similar measurements were repeated in 2002, but using a commercial CD-SEM operated under fabrication facility conditions.[9] An example of the agreement obtained is shown in Fig. 5.

The materials of greatest industrial interest are polysilicon and various resists, polysilicon because the smallest critical features in the manufactured end product are polysilicon transistor gates and resist because measurements prior to etch (when the sample consists of resist on as yet unpatterned polysilicon) are used in process control. Polysilicon also has advantages from the standards point of view, because resist is dimensionally unstable, an important disadvantage in a dimensional standard. Because of this and because there are other problems in measuring resist, polysilicon samples were deemed more suitable test samples during development of the MBL method. For this reason, the studies referenced above all made use of polysilicon samples.

With successful completion of those projects, attention turned in the current project to resist. Resist shrinks upon electron beam exposure. It is insulating, so it accumulates charges that may affect the trajectories of subsequently produced secondary electrons. Certain of its properties (e.g., its plasmon resonance energy) that influence the

secondary electron yield are only poorly known, making modeling it more uncertain. It was not known at the inception of this project whether these issues represent only annoyances or insurmountable obstacles to good CD metrology. The purpose of this project is to attempt measurements on resist patterns using the MBL technique.

The general approach is similar to our previous projects with polysilicon samples. Resist samples were measured top-down in the CD-SEM. From these images, the sample cross-section was determined using the MBL method. These samples were cross-sectioned as close as possible to the area that had been imaged top-down. These cross-sections were imaged and the profiles determined from them. The widths determined by MBL were compared to the widths determined directly by cross-sectioning.

2 EXPERIMENTAL

The test pattern used for this project is shown schematically in Fig. 6. This pattern is one of many on the AMAG4L reticle at ISMT. ISMT fabricated samples consisting of 290 nm high developed PAR-810 resist lines on 80 nm of ARC29A in a focus-exposure matrix. Within this matrix, measurement targets were located at the positions shown in Fig. 7. Within each die, targets were located in the regions labeled A, C, and E in Fig. 6, corresponding to 100 nm, 200 nm, and 350 nm lines respectively. Within each of these regions there were both low magnification and high magnification targets, as shown in Fig. 8.

The top-down images were acquired on ISMT's Applied Materials NanoSEM using a landing energy of 500 eV and a beam current of 10 pA. The high magnification areas imaged were predosed with a 1000 eV electron beam, 4.5 μs of dwell time per pixel, with 1024 linescans of 960 pixels each. The purpose of predosing the sample was to pre-shrink the lines, thereby reducing shrinkage of the resist during subsequent images. The high magnification images were taken with 992 × 128 pixels, a beam current of 10 pA, and a pixel dwell time of 2.3 μs. The imaged area was 2.69 μm × 2.1 μm. These parameters result in an image pixel that is about 6 times larger in the vertical dimension than in the horizontal. This was done to reduce the electron beam exposure as much as possible without compromising the instrument's resolution in the important direction perpendicular to the lines, which were oriented in the vertical direction as shown in Fig. 9.

The goal of the cross-sectioning was to cleave the sample through the area that had been imaged top-down. These areas were quite small, on the order of 2 μm square as indicated above, but still within the 1 μm specification of the Sela cleaving tool. However, that specification may not have anticipated the need to stay within 1 μm over a distance sufficient to cleave all three sets of targets indicated in Fig. 6. Had we been able to cleave through the imaged areas it might have been possible to determine the precise relationship between the cleavage line and the top-down image. Unfortunately, it does not appear that this was successful in general. Figure 10 demonstrates that the cleavage lines sometimes missed their target direction by several micrometers, as a result of which at best only some of the cleaves could have gone through the imaged areas. This means our top-down information and cross-section information derive from different parts of the same line, and may differ from one another due to line width roughness. The cross-section images were 2560 × 1920 pixels with a 2.56 μm × 1.96 μm field of view and 1 keV landing energy. A typical image is shown in Fig. 9.

3 ANALYSIS

3.1 Generation of resist libraries

MONSEL was used to simulate SEM images of resist lines at 500 eV landing energy. The edges were parameterized as shown in Fig. 2. We simulated all combinations of four radii (0 nm to 60 nm with a 20 nm increment), six angles

(0° and 1° to 9° in 2° increments), five line separations (isolated, 100 nm, 200 nm, 300 nm, and 500 nm) and two secondary electron extraction efficiencies (0 % and 100 %). (CD-SEMs often use electric fields to extract secondary electrons. These fields deflect electron trajectories up and away from the sample, thereby allowing electrons to be counted that would otherwise have collided with the sample and been reabsorbed. This parameter is a measure of the efficiency of this process.) Two of the input parameters required for the modeling, the densities of cured ARC29A and PAR-810 resist, were apparently not well known, either by resist engineers at ISMT or by the manufacturer of the materials. For this reason ISMT sent cured thin films of these materials on wafers to NIST, where the film densities were measured in the Polymers Division using x-ray reflectivity.[10] The resulting densities were 1.29 g/cm^3 and 1.26 g/cm^3 for ARC29A and PAR-810 resist respectively.

3.2 Assignment of MBL edge positions from top-down CD-SEM images

Of the images attempted, there were 48 pairs for which both the top-down and the cross-section images of dense line areas were successful. Each of the top-down images in these pairs was analyzed using the MBL method. For the fits, some parameters were pinned while others remained free. For example, as described above, the line separation was one of the library parameters. This parameter measures the distance between adjacent lines. The measured profile is sensitive to this, particularly when extraction fields are small, because some secondary electrons that escape from the sidewall of one line are captured when they hit the sidewall of a nearby line. For line separations of 100 nm or more, as is the case for these samples, the predicted profile does not differ significantly for separation changes of a few nanometers. For this reason, edge position uncertainty at the level of a few nanometers is not important for the selection of the appropriate separation parameter. For each image, the parameter was therefore pinned to the average value appropriate for that sample, as determined from the image. A subset of linescans in each image was analyzed in a single fitting operation with both instrument and sample parameters free. The instrument parameters (beam diameter, contrast, brightness, and extraction efficiency) were pinned to the values determined from this fit. The remaining fits were performed one scan line at a time with only three free parameters per edge. These parameters were the edge position, sidewall angle, and top corner radius. The bottom edge positions determined by a typical fit are shown in green in Fig. 11. The linewidth roughness can be determined from these edge curves. It averaged about 3 nm (root mean square) for all lines, independently of linewidth.

3.3 Modeling and edge assignment for cross-section SEM images

To complete the comparison, edge positions must also be assigned to the cross-section images. These images are also subject to blooming at the edges, as is evident in Fig. 9. MONSEL is capable of modeling sample geometries that can be described by roughly trapezoidal lines on a one to three layer substrate. Fortunately, the cross-section geometry can be treated as a special case of such a sample, one in which the "line" is very tall and the three "substrate" layers are either of 0 thickness or comprised of vacuum (Fig. 12). This was simulated in MONSEL for incident electrons at 1 keV, the energy used by ISMT for the cross-section images, and with beam cone angles varying from 0° to 0.8°. Corner radii and sidewall angles were zero, because this is what we expect for the cross-section geometry. In principle, the edge positions of the cross-section image might have been determined by fitting the observed profiles to this simplified library. However, as can be seen in Fig. 9, there was an artifact near the base of the lines in the cross-section images that manifested itself as a bright region adjacent to the line edges. This artifact is most likely some out-of-focus structure near the end of the line, several micrometers below the cleavage plane. It is visible in the image because of the SEM's large depth of field. Unfortunately, this structure complicates fitting a library profile to the measured profile. Instead, we determined the position of maximum intensity from the cross section image, and then added to this an offset in order to assign the edge position. The offset associated with various beam cone angles was determined by the modeling already described, and is shown in Fig. 13. As is evident in that figure, the offset from the maximum brightness to the true edge position is a sensitive function of the beam cone angle. The shape of the cross-section SEM profiles near the line tops, where the influence of the previously mentioned artifact near the base was minimal, was most consistent with a beam divergence half angle of about 0.2°. At this beam half angle, the true edge position is slightly less than 1 nm away from the position of maximum bloom brightness, in the direction away from the line center. This was the offset we used to assign edge positions to the cross-section images. However, because of the sensitivity of the assignment to beam divergence, there is a

substantial amount of uncertainty associated with this. If we assume the true divergence angle lies between 0° and 0.8°, then the offset, which we have taken to be approximately 1 nm, might lie anywhere between -3 nm and +5 nm. The sensitivity in cross-section images is much greater than for top-down images because the effective height of the line is so much larger (Fig. 12). When the beam diverges, parts of it still strike the sidewall even when the central beam position is considerably beyond the edge. This is unlike the situation in a top-view. In that view, the substrate is only a few hundred nanometers below the top surface where it can intercept all of the electrons as soon as the beam is aimed a few nanometers beyond the edge.

3.4 Comparison of MBL and cross-section results

The result of each of the edge position determinations described above is a set of data describing the edges in each image. The MBL parameters include the position where each edge intersects the substrate and the angle of the edge. From these parameters a profile for that line was computed. To compare the MBL-derived profiles to the cross-section ones, it is necessary to compensate for any magnification difference between the CD-SEM and laboratory SEM tools. Since our samples are periodic arrays of lines, this was done by scaling one of the images until the periodicity of the lines was the same as that in the other image. (The result of this operation indicated that the CD-SEM and laboratory SEM scale calibrations differed from one another by 0.8%. This difference was consistent across all of the periodic image pairs.) After putting the results on the same scale, the profiles were shifted with respect to one another in the *y* direction in order to make the position of the top of the substrate match, and in the *x* direction by an amount determined to produce the best fit between the two.

Three of the 48 such comparisons are shown in Fig. 14. With the goodness of fit judged by the sum of squares of the differences between the edge locations, these three represent a good fit (90'th percentile), median fit (50'th percentile), and a bad fit (10'th percentile) in order to convey both the typical agreement and the amount of variation around that typical result. All of the examples shown here were taken from the nominally 100 nm features (which were actually approximately 69 nm after developing). However, the results for the wider lines (nominally 200 nm and 350 nm) were similar.

Quantitatively, the extent of agreement can be judged by determining the average top to bottom width of each line from the MBL results and from the cross-section images. We begin by computing a set of residuals, $\Delta w_i = w_{\mathrm{MBL}i} - w_{\mathrm{xs}i}$. The *i*th residual is the difference between the MBL result and the cross section result for the *i*th line. Each of our 48 targets had more than one line, resulting in 284 residual values in all. The average residual was 3.5 nm, as shown in the third column of Table 1. This offset indicates that one or the other method (or a combination of both) has this much measurement bias. At the scale of our images, this bias amounts to approximately 1 image pixel on each edge of a line. There are two quite plausible sources of measurement bias that could account for this much difference. The first is error associated with the beam divergence angle. (Recall the discussion associated with Fig. 13.) The second is shrinkage of the resist due to electron beam exposure, a known phenomenon.[11,12] Notice that the MBL result is systematically larger than the cross-section result (i.e., the table entries are positive). This difference has the correct sign: the cross-section images were taken after the MBL top-down images and were therefore subjected to an additional e-beam exposure, any shrinkage from which would tend to make them narrower than the MBL result. Either of these effects could easily account for the observed difference.

In addition to the measurement bias just described, there is also a random difference between the two determinations. That is, the difference between the MBL and cross section results for a particular line might be more or less than the average difference discussed in the last paragraph. The standard deviation of the residuals was about 5 nm, as shown in the last column of Table 1. In discussing the sources of this random error, it is convenient to divide it into two components.

One component is the variance within each cross-section image (i.e., within-target). In Fig. 14b, for example, there are ten lines, each of which has an associated residual. The standard deviation of these was close to 3 nm for all the

different width targets, as can be seen in the table's 4th column. This variation can be understood in terms of the line width roughness (LWR). The cross-section represents a particular slice through the line. The width there is expected to differ from the average width by an amount characterized by the LWR. We measured the standard deviation in linewidth on these samples from the top-down images to be 2.9 nm. We therefore expect 2.9 nm of variation from this source, an amount that corresponds quite closely to the observed value.

This component of variance does not capture all of the variation because the standard deviations are computed with respect to each target's own average residual. These within-target averages vary from one target to the next. Since there is within-target variation, a certain amount of target to target variation is expected simply due to sampling, but such variation should be smaller by a factor of $\sqrt{3}$ to $\sqrt{10}$ since there are 3 to 10 lines within each image (three 350 nm lines, five 200 nm lines, or ten 100 nm lines depending upon the target). Since the within-target variation is only about 3 nm, this is 1 nm to 1.7 nm, not large enough to explain the roughly 4 nm of variation observed and reported in column 5 of Table 1. The source of this variation remains somewhat mysterious. It is not a truly systematic error (as a faulty assumption about the instrument's beam divergence would be for example) because it is not the same for all targets. Neither is it completely random, since it would then show up in the within-target component. Rather, it is a systematic component that is associated with individual targets and varies from target to target. Some possible sources of variation that would behave this way include: 1) Target to target variations in the amount of charging or resist shrinkage due to inconsistent exposure of the targets during set-up and focusing. (This is possible since the cross-section image acquisition in the ISMT FA lab is a manual procedure.) 2) Target to target variation in focus. The entire image is acquired at a single focus setting, but when the sample is changed the instrument must be refocused. MBL is meant to compensate for focus variation in the top-down images, but this would not apply to the cross-section images. 3) Since the top-down and cross section images were taken at different parts of the line, the possibility that the lines all tend to be larger or smaller at the second location cannot be eliminated in principle, though it is not clear what would be the source of such correlation—perhaps local variations in the etch rate or optical effects.

Table 1: Agreement between MBL and Cross-Section Results

Nominal Linewidth (nm)	Actual Linewidth (nm)	Average w_{MBL}- w_{xs} (nm)	Random Error (nm)		
			σ (within target)	σ (target to target)	σ (total)
100	62.1	3.2	2.6	3.2	4.1
200	166.6	4.0	3.2	5.5	6.2
350	316.7	3.3	3.7	4.0	4.7
All lines	—	3.5	3.2	4.4	4.9

4 CONCLUSIONS

The average linewidth of resist lines derived from top-down CD-SEM images using the model-based library (MBL) approach agreed with widths derived from cross-sections to within the uncertainty of the comparison.

There were random differences between the widths determined by the two techniques. This difference had a standard deviation of approximately 5 nm. Of this, 3 nm is expected due to line width roughness.

There was also a systematic difference of 3.5 nm between the cross-section and MBL determinations. This much difference (about 1 image pixel per edge) could be accounted for by an error in the cross-section edge assignment

associated with the electron beam divergence angle (i.e., depth of field) being different from what we assumed or it could be caused by shrinkage of the resist due to electron beam exposure.

The sensitivity of the cross-section determination to the SEM's depth of field is a significant unexpected finding of this study. It represents a heretofore unappreciated error source for determining widths from SEM of sample cross-sections. This points to the need for the development of appropriate electron beam shape measurement methods.

The effect of charging upon dimensional metrology has been a matter of concern when dealing with resist samples. The size of the effect has not been known, and the possibility that charging might render good model-based SEM metrology of resists difficult or impossible was a real one. It is possible that some of the unexplained random difference between MBL and cross section results, or some of the systematic difference between them, could be accounted for by effects due to charging or shrinkage. While some such effects cannot be ruled out, the size of the disagreement between MBL and cross-section measurements presented here places an upper bound of at most a few nanometers on the size of those effects. It is possible they were smaller than this, if other phenomena were responsible for these residual differences.

ACKNOWLEDGMENTS

Funding for this project was shared by International SEMATECH, the NIST Office of Microelectronic Programs, and the NIST Manufacturing Engineering Laboratory. At International SEMATECH, Michael Bishop, Ben Bunday, and the staff of the ISMT FA lab contributed to sample fabrication, image acquisition, and sample cleaving. Dr. Eric Lin, in NIST's Polymers Division, arranged for measurements of the densities of the resist and BARC materials used in our samples.

REFERENCES

1. International Technology Roadmap for Semiconductors, (Semiconductor Industry Association, 2003), Table 117a, Metrology Section, pg. 10.
2. J. S. Villarrubia, A. E. Vladár, M. T. Postek, "A simulation study of repeatability and bias in the CD-SEM," Proc. SPIE **5038**, pp. 138-149, 2003.
3. V. A. Ukraintsev, "Effect of Bias Variation on Total Uncertainty of CD Measurements," Proc. SPIE **5038**, pp. 644-650, (2003).
4. J. R. Lowney, A. E. Vladár, and M. T. Postek, "High-accuracy critical-dimension metrology using a scanning electron microscope," Proc. SPIE 2725, pp. 515-526, 1996; J. R. Lowney, "Application of Monte Carlo simulations to critical dimension metrology in a scanning electron microscope," Scanning Microscopy **10**, pp. 667-678, 1996.
5. M. P. Davidson and A. E. Vladár, "An inverse scattering approach to SEM line width measurements," Proc. SPIE **3677**, pp. 640-649 (1999).
6. "Edge Determination for Polycrystalline Silicon Lines on Gate Oxide," J. S. Villarrubia, A. E. Vladár, J. R. Lowney and M. T. Postek, Proc. SPIE **4344**, pp. 147-156, (2001).
7. J. S. Villarrubia, A. E. Vladár, and M. T. Postek, "Trial Shape-Sensitive Linewidth Measurement System," final report to International SEMATECH, 2001.
8. J. S. Villarrubia, A. E. Vladár, J. R. Lowney, and M. T. Postek, "Scanning electron microscope analog of scatterometry," Proc. SPIE **4689**, pp. 304-312 (2002)
9. J. S. Villarrubia, A. E. Vladár, and M. T. Postek, "Test of CD-SEM Shape-Sensitive Linewidth Measurement," final report to International SEMATECH, 2002.

10. Wen-li Wu et al., “Properties of nanoporous silica thin films determined by high-resolution x-ray reflectivity and small-angle neutron scattering,” J. Appl. Phys. **87**, pp. 1193-1200, (2000).
11. Habermas, A et al, "193nm CD Shrinkage under SEM: Modeling the Mechanism" Proc. SPIE **4689**, pp. 92-101 (2002).
12. N. Sullivan et al, "Electron Beam Metrology of 193 nm Resists at Ultra Low Voltage" SPIE **5038**, pp. 483-492 (2003).

FIGURES

Fig. 1. Edge assignment uncertainty: The finite width of the edge in a scanning electron microscope (SEM) profile of a line results in uncertainty concerning the proper edge assignment. The two rectangular lines beneath the image profile both have edges within the bloom regions and so are a priori equally plausible, but they differ in width by 10 nm.

Fig. 2. Parameterization of a polysilicon line: Seven geometrical parameters and three instrument parameters are indicated.

Fig. 3. Schematic operation of model-based library measurement. The measured SEM signals from each edge of the unknown sample are compared to signals in the library to determine the parameters that produce the best match. (The library only contains right edges, which are reflected left to right when matching to measured left edges.) The parameters include some affecting edge shape in addition to edge positions, so some shape information is obtained from the image in addition to the CD.

Fig. 4. Edges (smooth wide trapezoid, red in color versions of this document) deduced from top-down image using the model-based library method compared to edges (thinner noisier line, blue) deduced from the cross section image on which both are overlaid.

Fig. 5. Example result of comparison of MBL determined cross section (smooth trapezoidal line on or near the Si-vacuum interface, light blue in color versions) determined from a CD-SEM top down measurement performed using a commercial CD-SEM at ISMT. The linescan from the CD-SEM measurement is shown in white. The profile determined from the top down measurement is overlaid on a cross section image measured later. As usual, the cross section may have missed the target location by a small amount, and this may account for the remaining small differences between the profiles.

Fig. 6. Schematic of NIST 2120 test pattern on AMAG4L reticle. Measurement targets are inside of the red boxes.

Fig. 7. Measurement patterns were located in the numbered die of this focus-exposure matrix.

Fig. 8. The 100 nm "A" area of the NIST 2120 test structure. There is a 2 μm pitch calibratible scale pattern on the bottom. Above that the black line segments on left and right indicate the line along which the sample is to be cleaved. The measurement targets are along that line. The colored labels, lines, and boxes are not on the wafer. Small shaded (red) squares indicate the high magnification image targets. The larger shaded (blue) boxes are areas of the low magnification images.

Fig. 9. Typical low magnification (left) and high magnification (upper right) images of nominally 100 nm lines. The images were acquired with rectangular pixels: linescan spacings were larger than pixel to pixel spacings within a line. As shown here the images have been stretched to compensate. The cross section image that corresponds to this sample is shown at the lower right.

Fig. 10. Optical image of a 100 nm test pattern. The large rectangular area is part of the 100 nm scatterometery array. The line along which the sample was cleaved is on the right. The two vertical (yellow) fiducial lines are parallel to one another, and demonstrate that the line of cleavage missed the desired direction, as a result of which the dense and isolated "fingers" are approximately 3 μm shorter at the top of the image than at the bottom.

Fig. 11. Result of MBL analysis of a top-down image of nominally 100 nm lines. Edge assignments are shown in color. The red lines (dark in noncolor reproductions), coinciding with the brightest pixel near each edge, were the initial estimates used as input to the MBL fitting algorithm. The algorithm reports the bottom edge position, shown in yellow (generally outside the brightest pixel assignments), based upon the best match to modeled edges.

Fig. 12. Cross section imaging geometry. The sample is oriented with the cleavage plane facing up. The usual top of the line (in the CD-SEM imaging geometry), the sidewall, and the substrate are labeled. The hourglass-shaped object is schematic of the SEM's electron beam impinging near the edge of the cleavage plane. Within MONSEL this geometry can be treated as though the cleavage plane is a line top, the sidewalls are vertical, and the line is now very tall. The absence of a substrate in the direction of the beam travel is treated by telling MONSEL the substrate is vacuum.

Fig. 13. The intensity near a tall vertical edge depends upon the beam divergence angle. The three curves are labeled with the beam divergence angle in degrees. As shown here, if the angle is between 0º and 0.8º the point of maximum intensity may be anywhere from 3 nm to the left of the maximum to 5 nm to the right.

Fig. 14. Comparison of edge positions assigned by the MBL method on the basis of top-down CD-SEM images (smooth red lines) with those assigned to the cross section image (noisier blue lines). The middle image (b) represents a typical match (i.e., 50'th percentile for goodness of fit). Half the time, agreement was better than this, and half the time it was worse. The top image (a) is at the 90'th percentile. (Only 10% of matches were closer.) The bottom image (c) shows one of the poorer matches—90% of the time agreement was better than this.

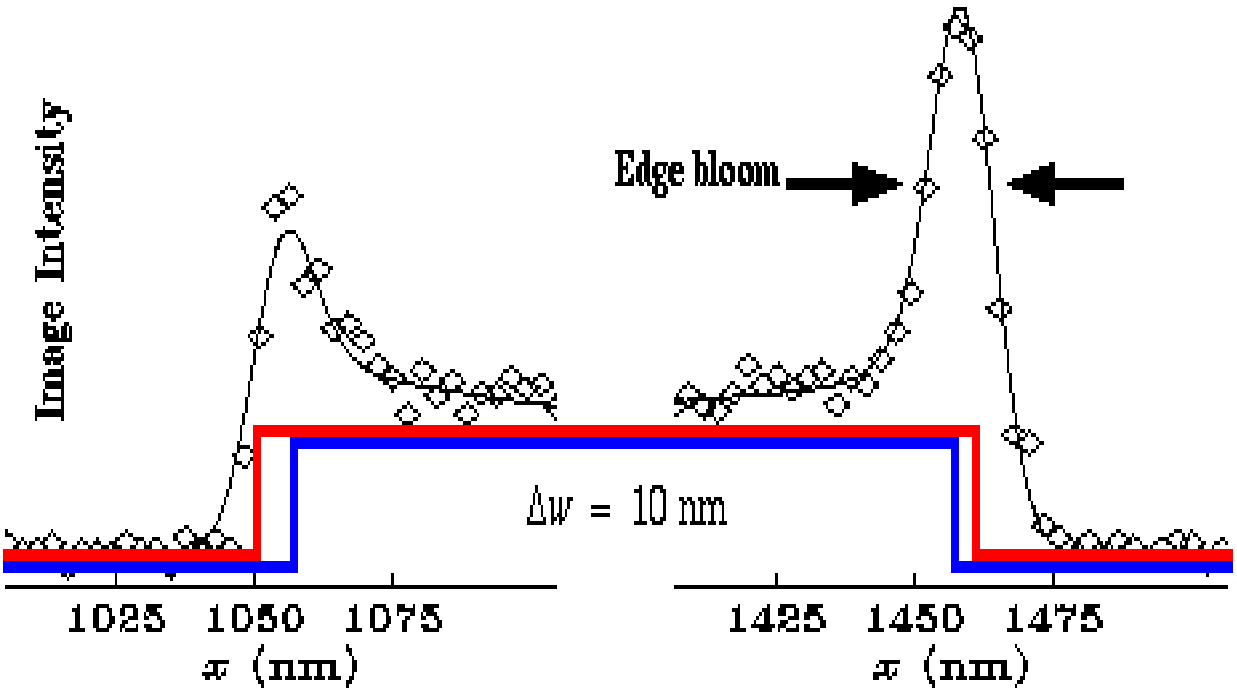
Image Intensity
Edge bloom
Δw = 10 nm
1025 1050 1075
x (nm)
1425 1450 1475
x (nm)

Figure 1

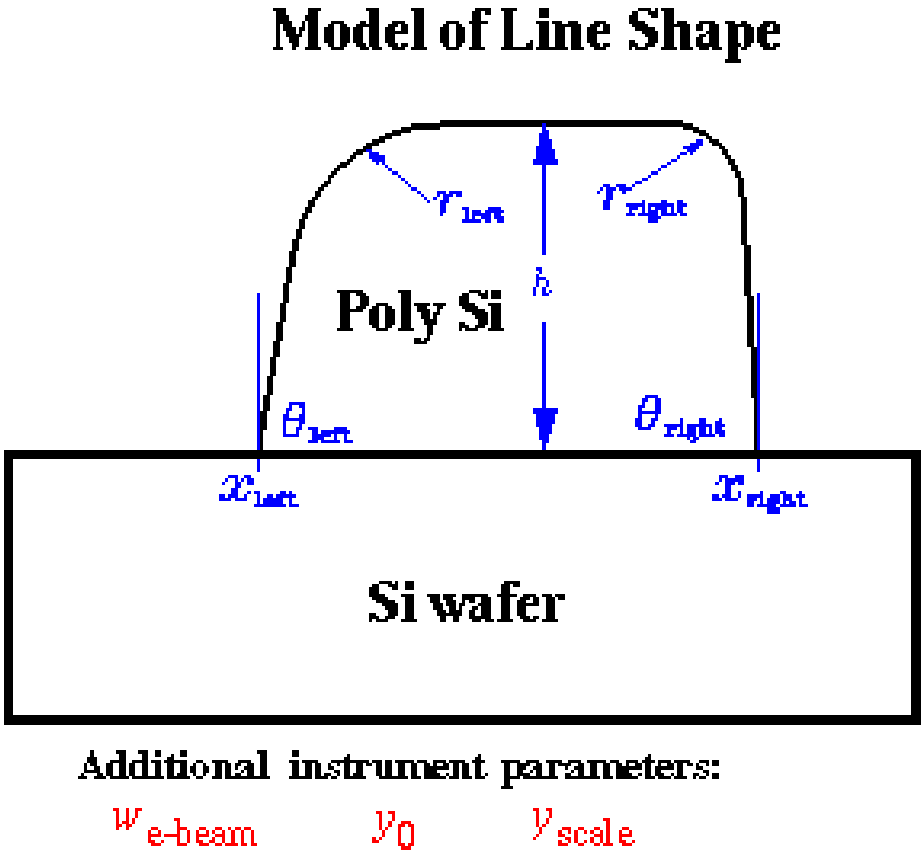
Model of Line Shape
r_{left}
r_{right}
Poly Si
h
θ_{left}
θ_{right}
x_{left}
x_{right}
Si wafer
Additional instrument parameters:
$w_{e\text{-}beam}$
y_0
y_{scale}

Figure 2

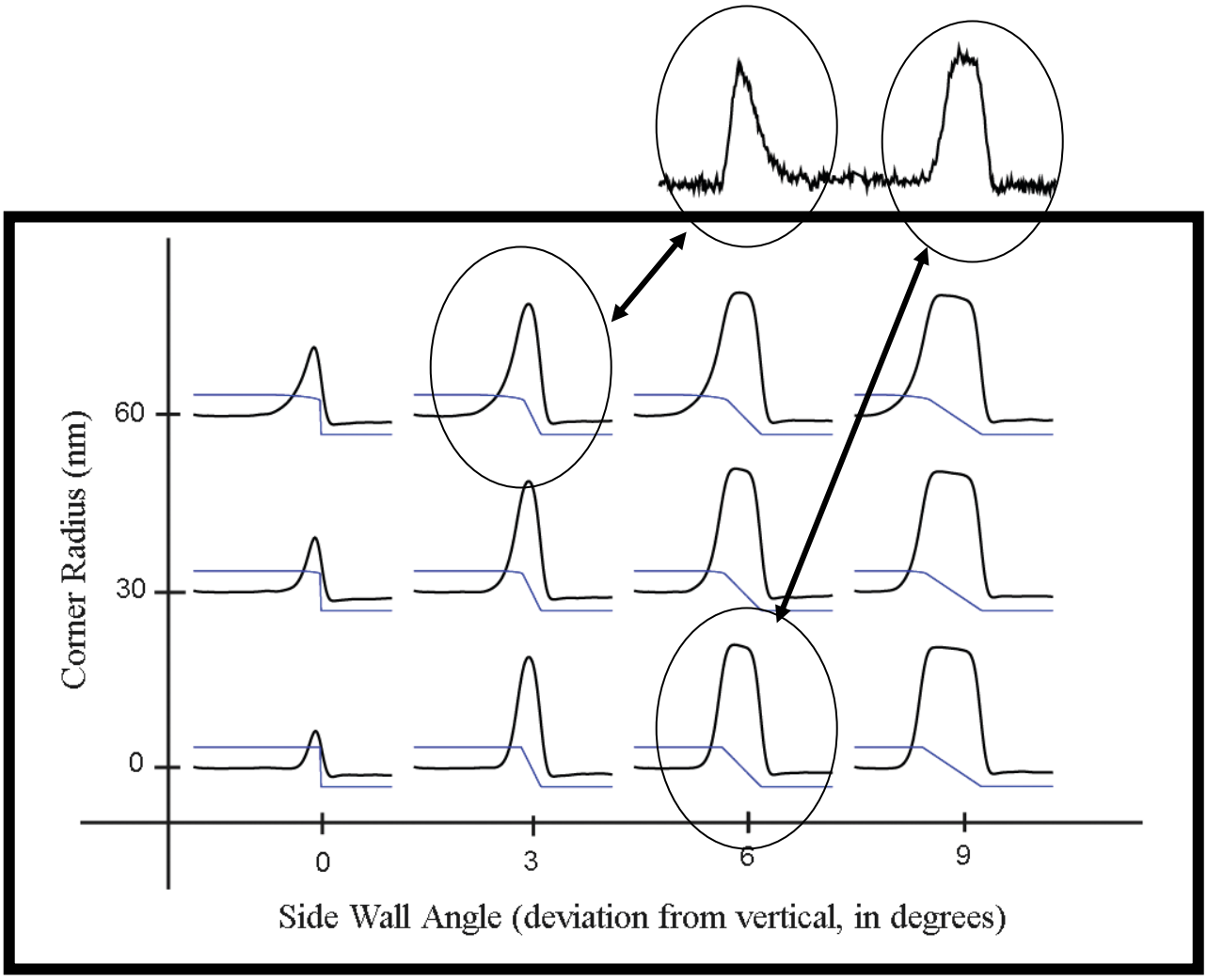
Corner Radius (nm)
60
30
0
0
3
6
9
Side Wall Angle (deviation from vertical, in degrees)

Figure 3

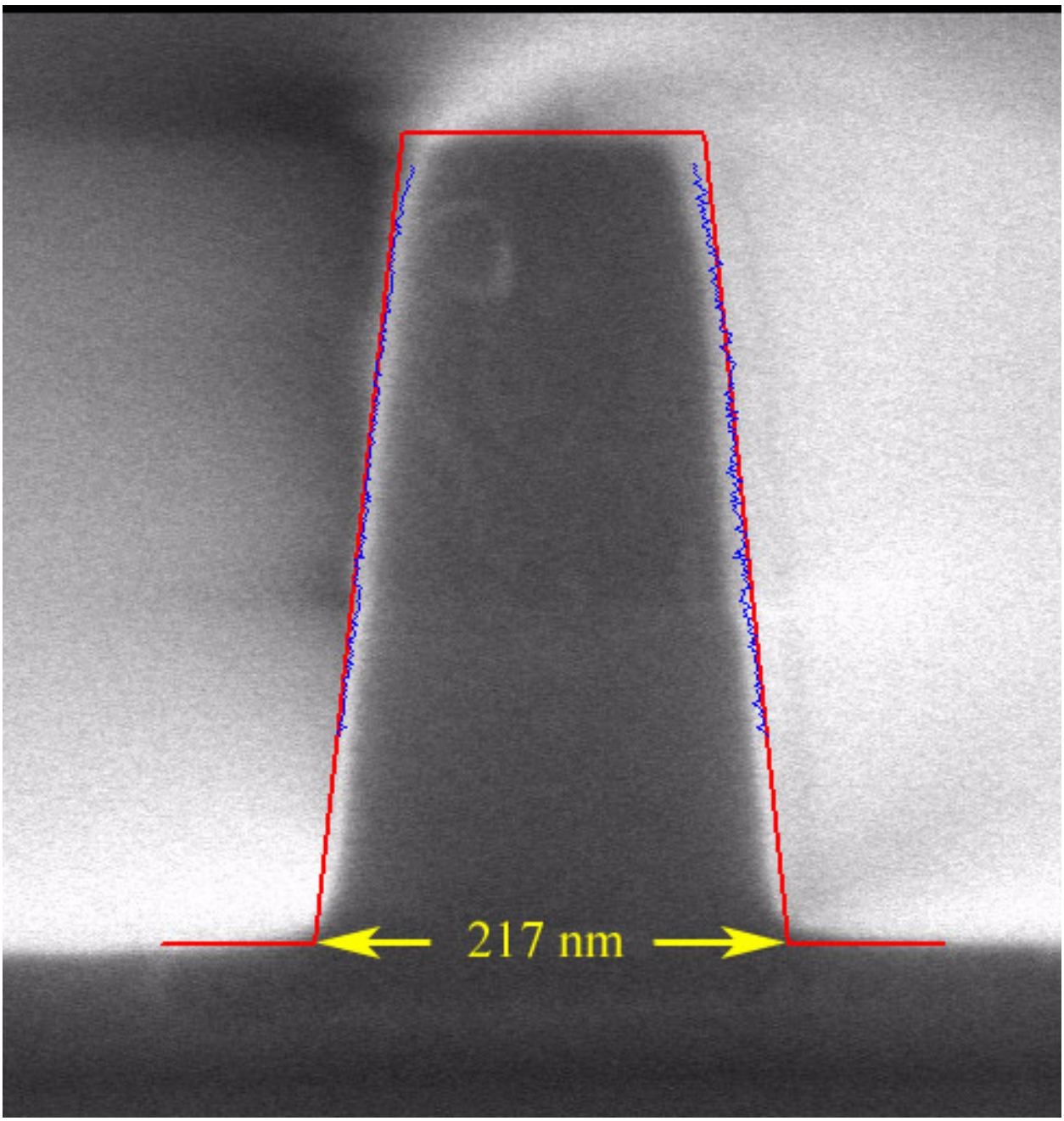

Figure 4

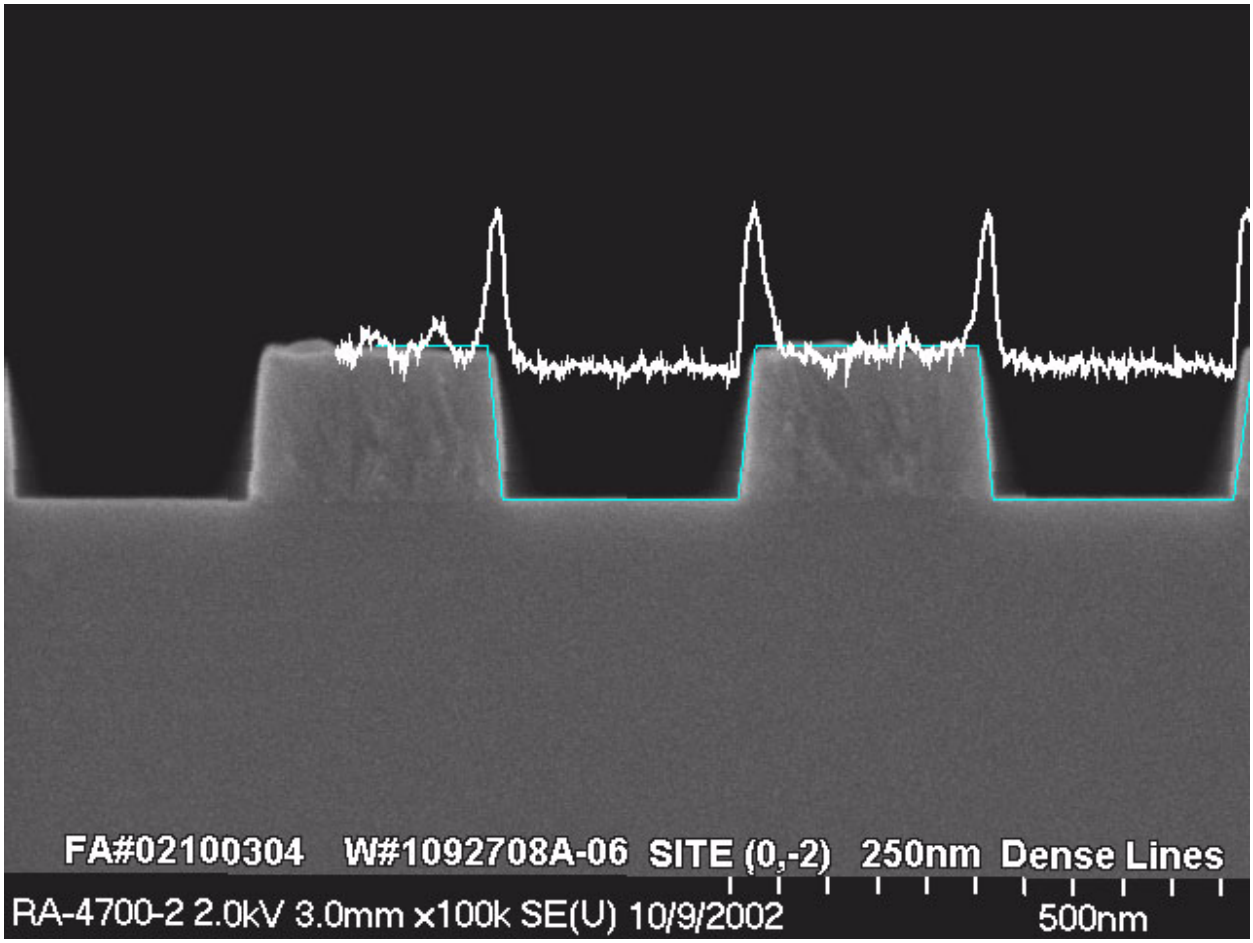
FA#02100304 W#1092708A-06 SITE (0,-2) 250nm Dense Lines
RA-4700-2 2.0kV 3.0mm x100k SE(U) 10/9/2002
500nm

Figure 5

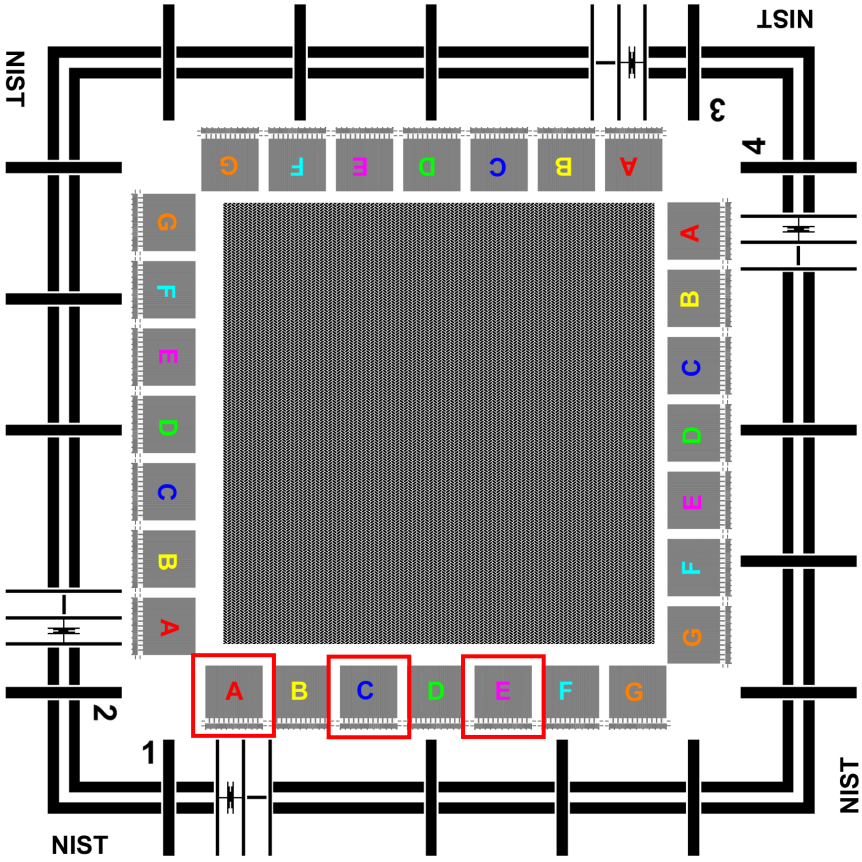

A 100 nm structure
B 140 nm structure
C 200 nm structure
D 250 nm structure
E 350 nm structure
F 500 nm structure
G 1000 nm structure

Equal lines and spaces within each structure!

250 nm crosses

Letter-labeled line width structure orientation rotates with the label, 1 and 3 vertical 2 and 4 horizontal

Black labels to be printed, colored ones NOT to be printed

Figure 6

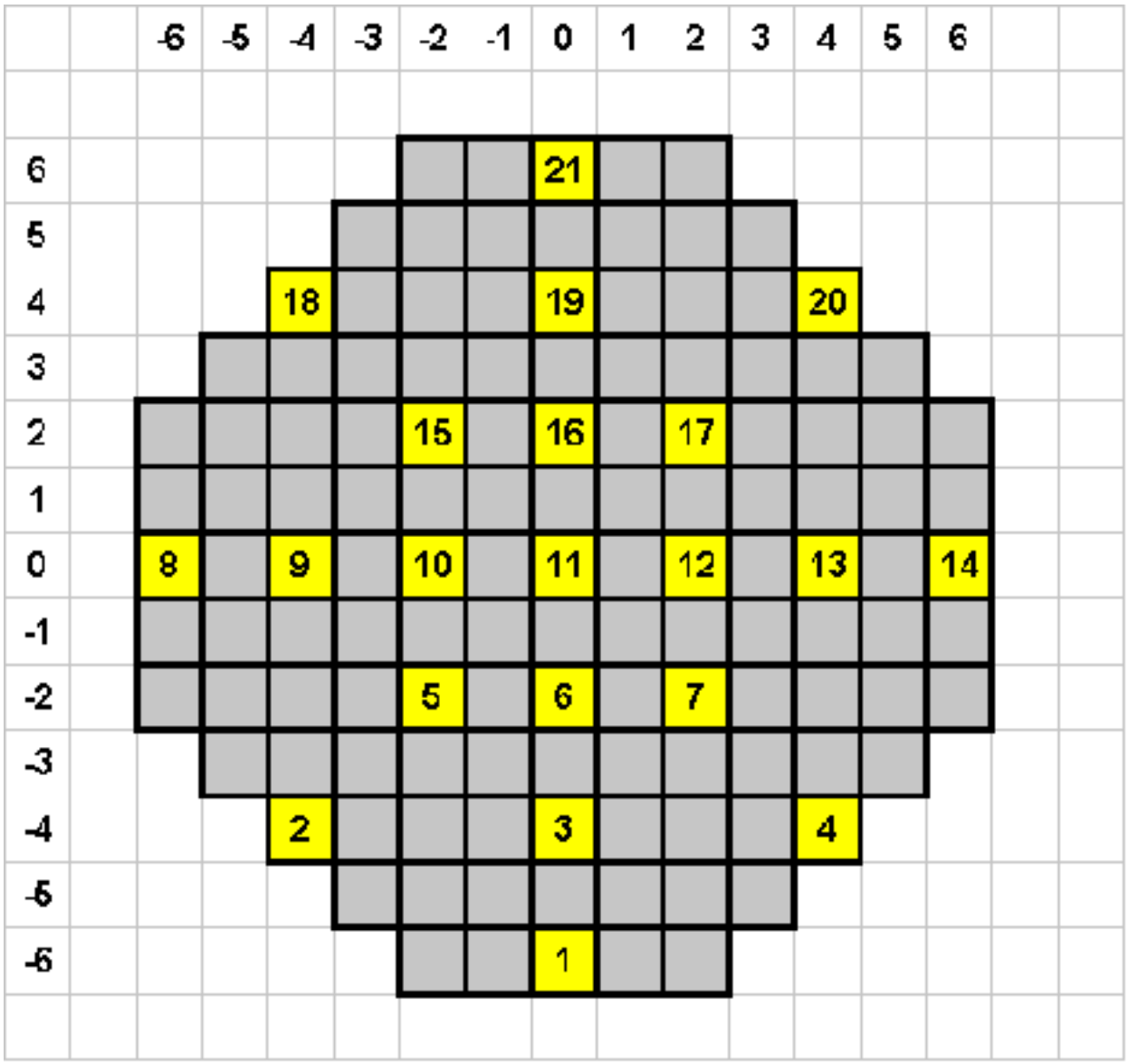
-6 -5 -4 -3 -2 -1 0 1 2 3 4 5 6
6 5 4 3 2 1 0 -1 -2 -3 -4 -5 -6
21
18 19 20
15 16 17
8 9 10 11 12 13 14
5 6 7
2 3 4
1

Figure 7

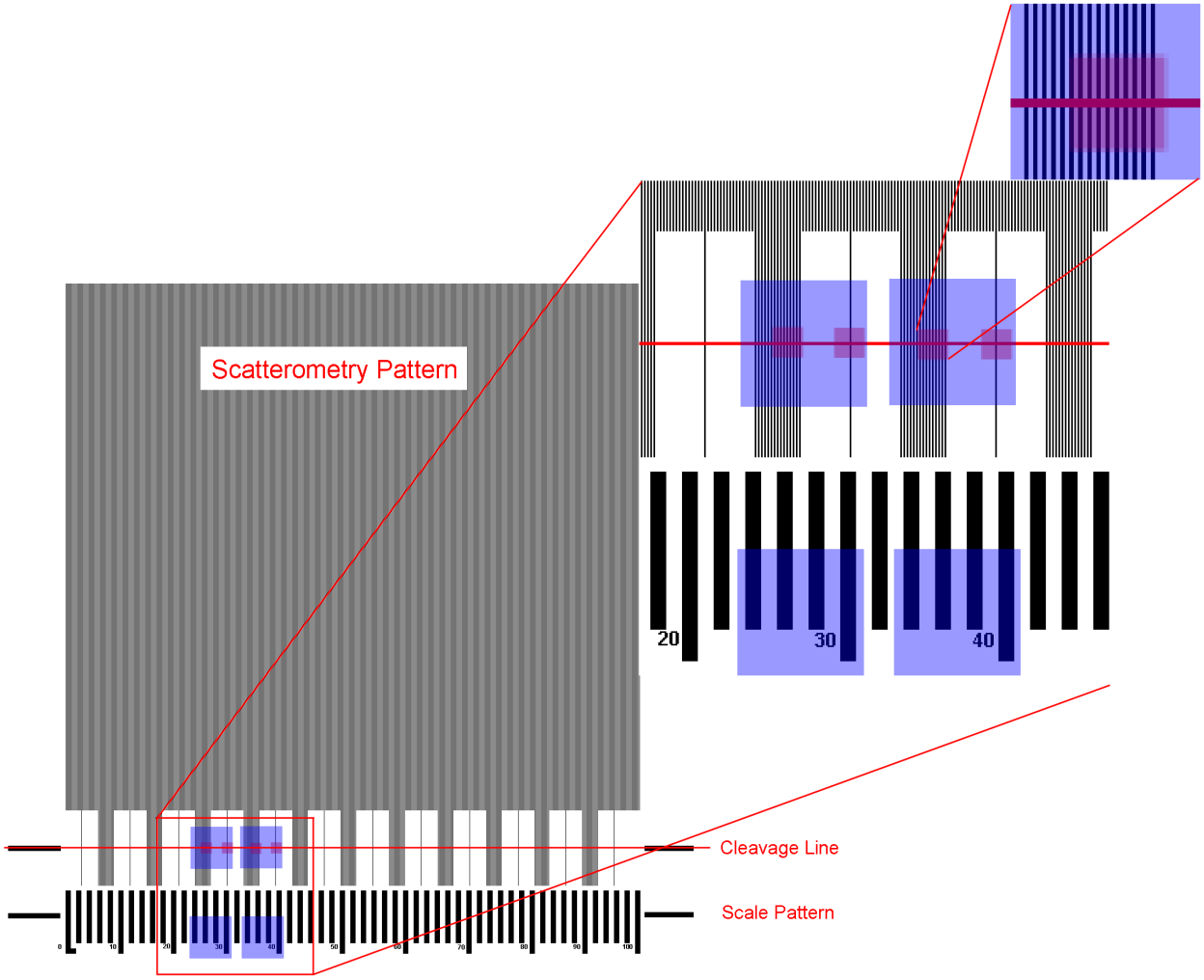
Scatterometry Pattern
20
30
40
Cleavage Line
Scale Pattern

Figure 8

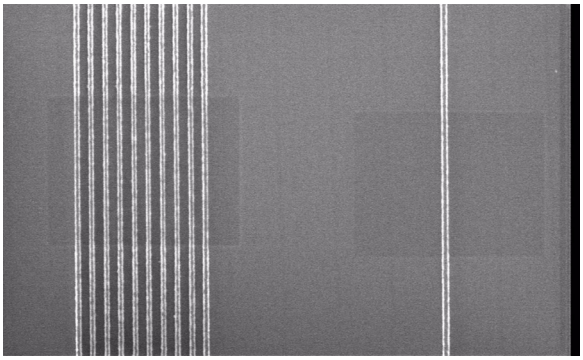

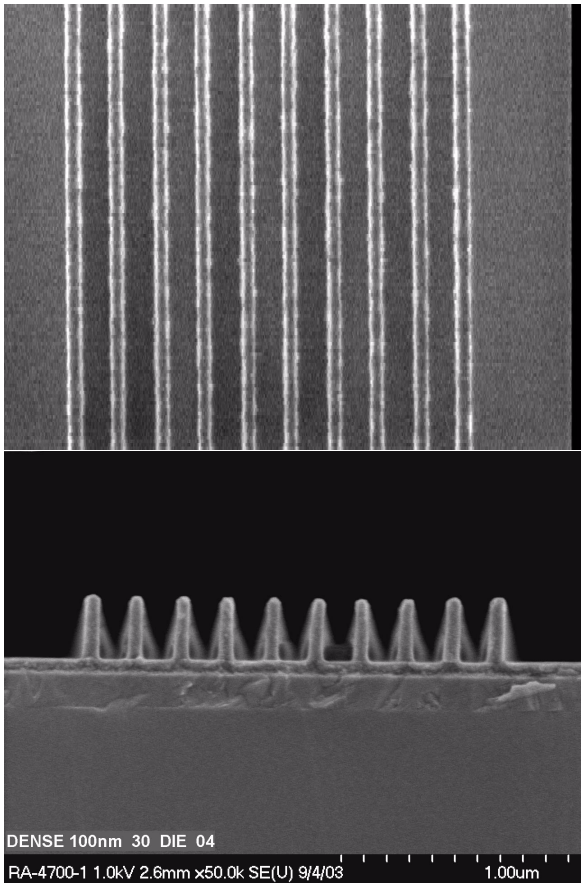

Figure 9

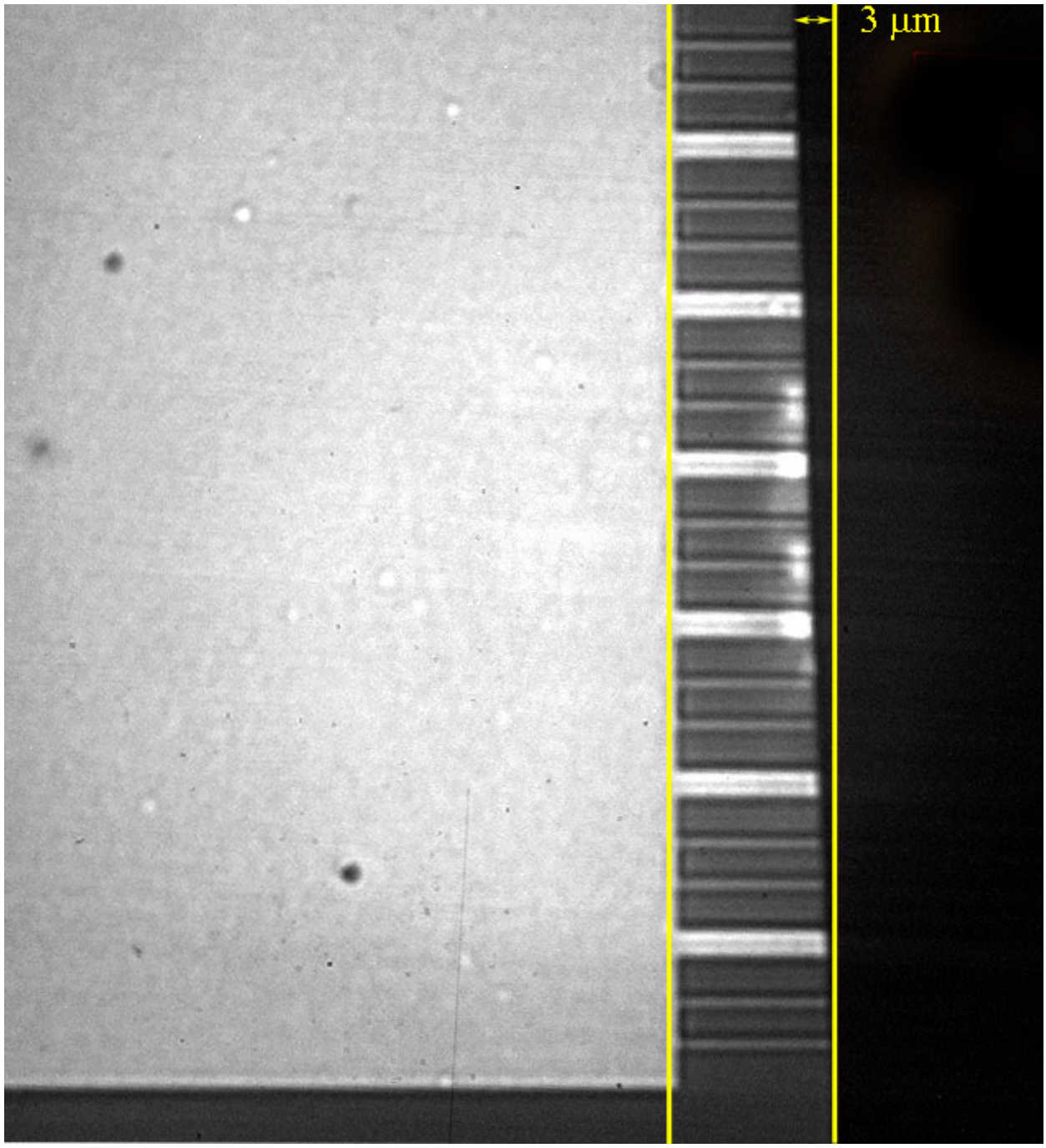

Figure 10

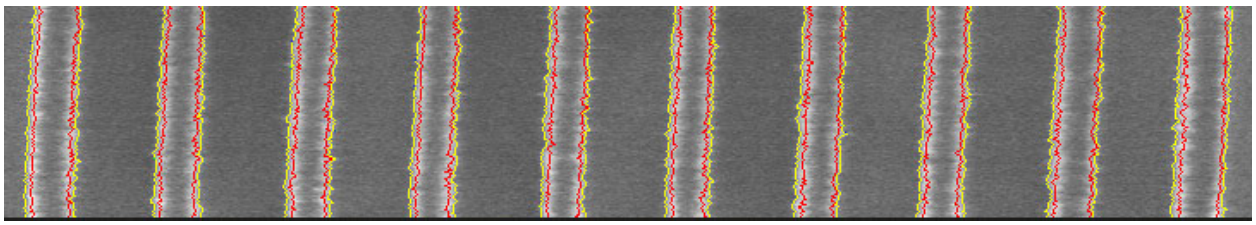

Figure 11

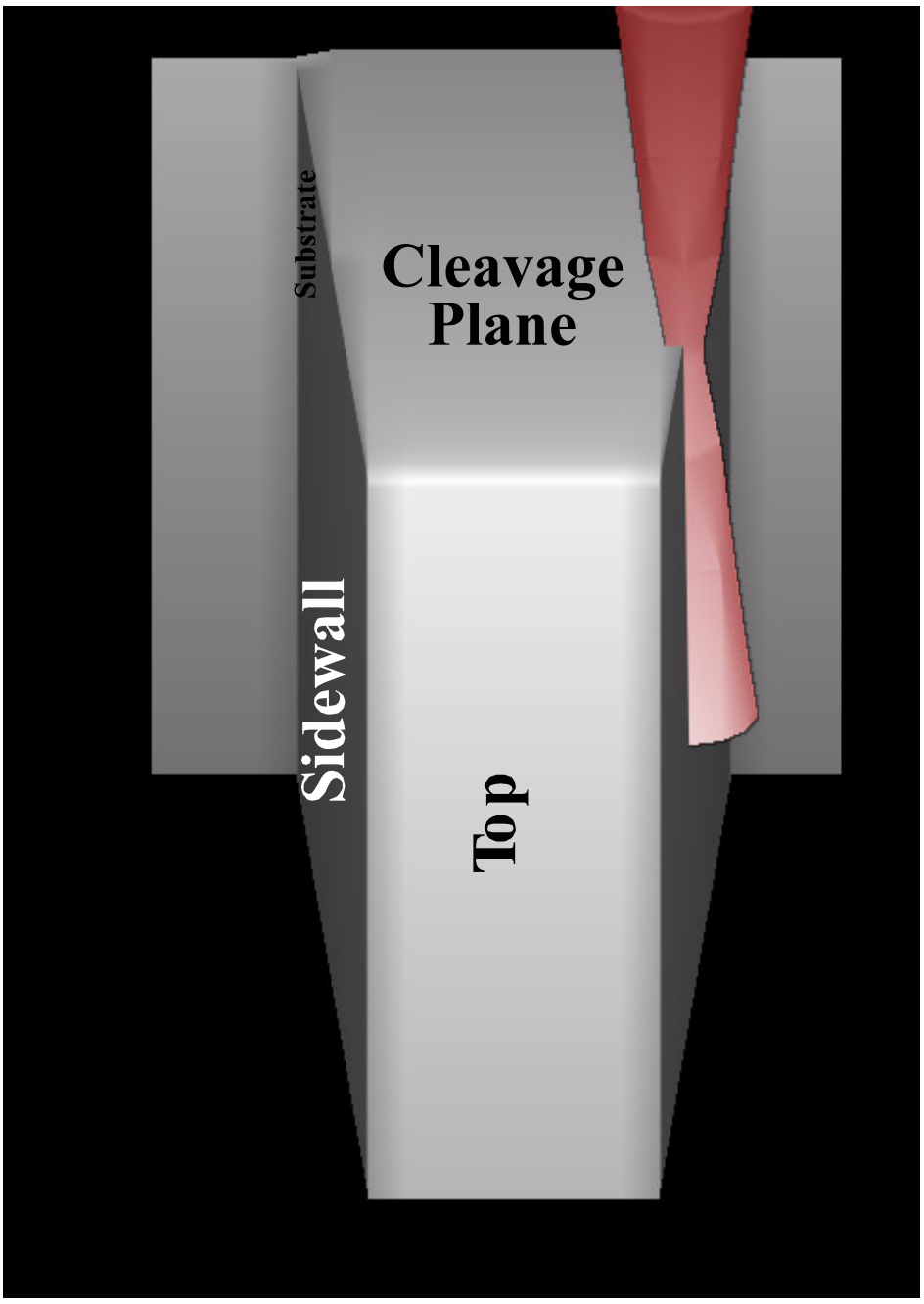

Figure 12

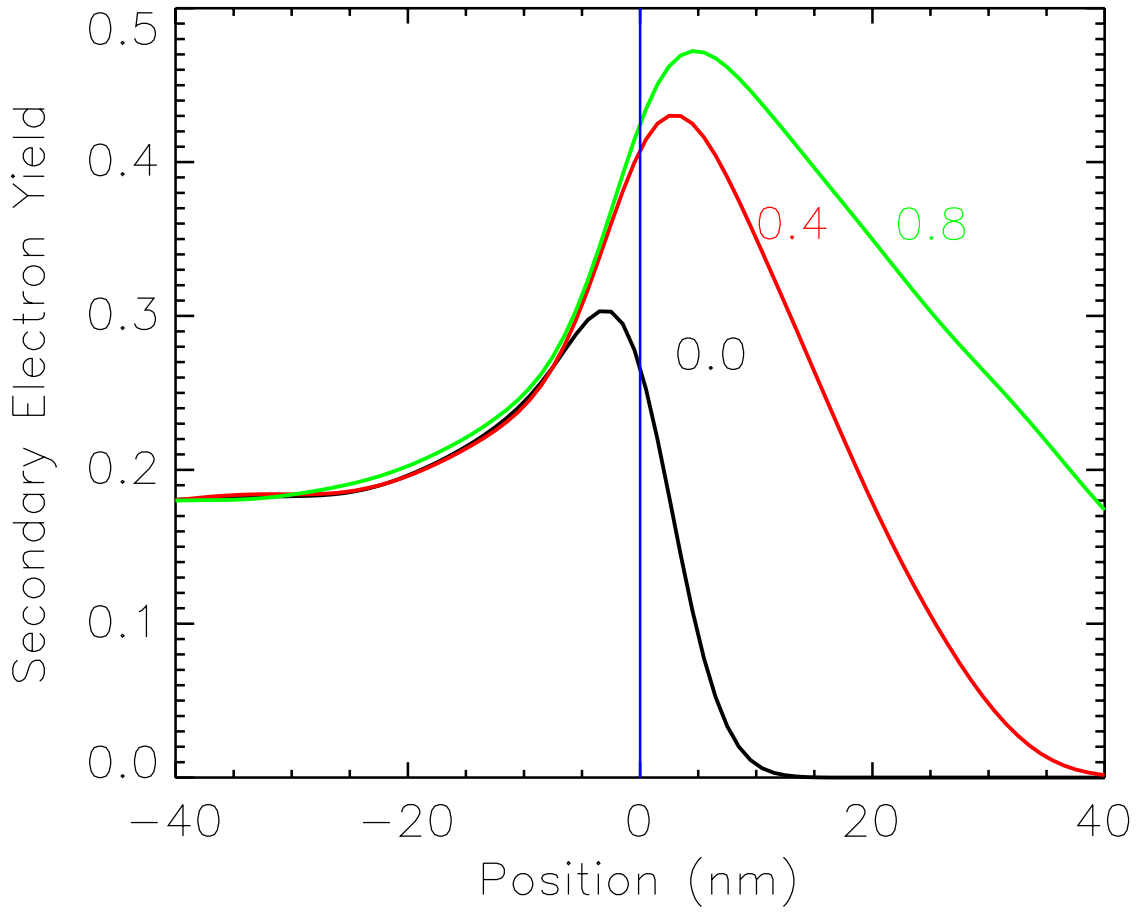
Secondary Electron Yield
0.5
0.4
0.3
0.2
0.1
0.0
−40
−20
0
20
40
Position (nm)
0.4
0.8
0.0

Figure 13

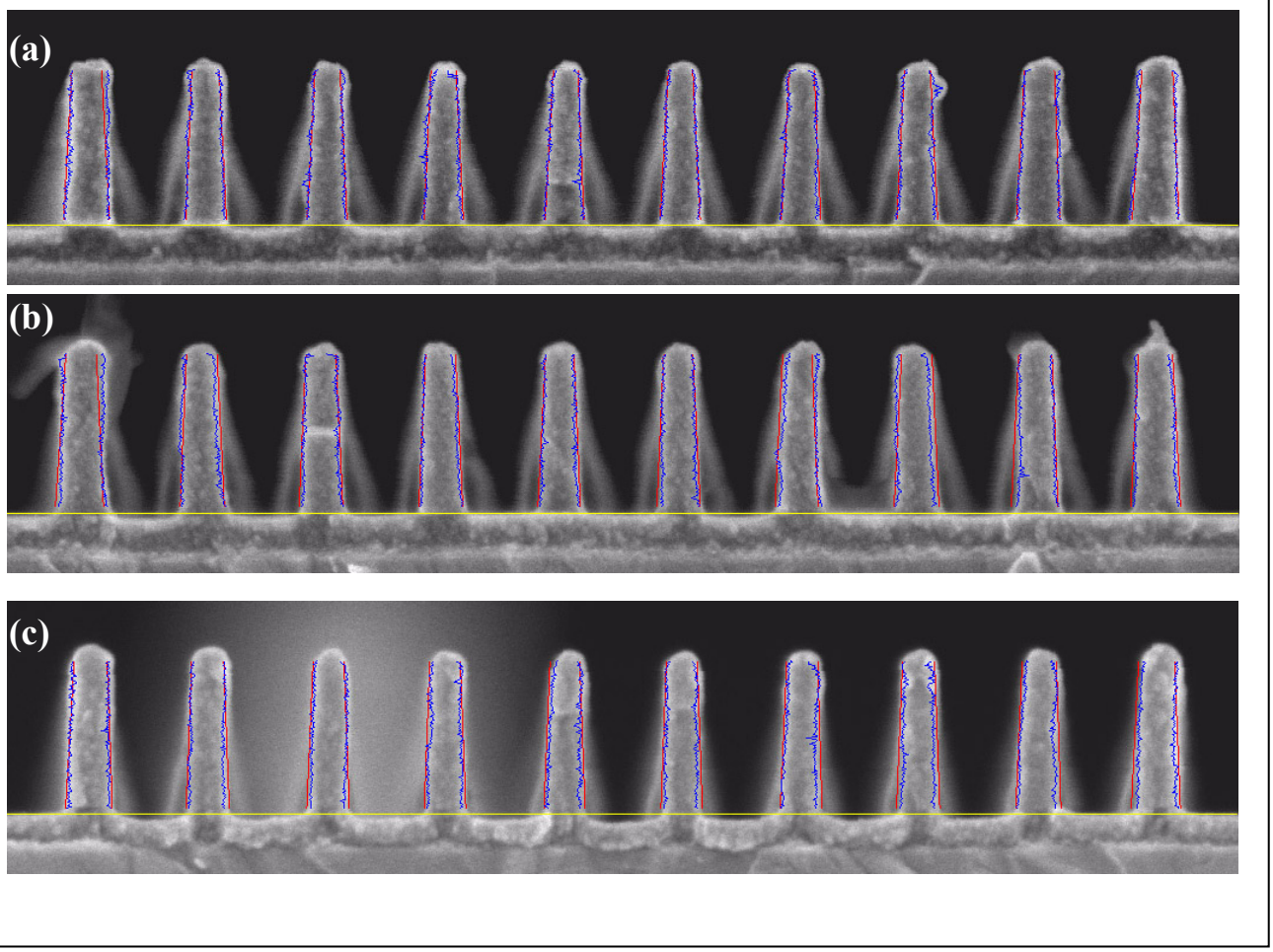

Figure 14

International SEMATECH Technology Transfer
2706 Montopolis Drive
Austin, TX 78741

http://www.sematech.org